Study of Spilled Oil Behavior on the Topsoil Induced by Thermal Diffusion

Nirmala P. Ratchagar
Annamalai University

S. V. Hemalatha
Annamalai University

Study of Spilled Oil Behavior on the Topsoil
Induced by Thermal Diffusion

[1]**Nirmala P. Ratchagar &** [2]**S.V. Hemalatha**

Department of Mathematics
Annamalai University
Annamalainagar - 608 002, India
[1]nirmalapasala@yahoo.co.in, [2]hemaazhagu@yahoo.com

Abstract

The fate and transport of oil spilled in soil has long been a focus for experimental and theoretical research in subsurface hydrology. Oil transport in the soil is affected by a large number of physical, chemical and microbial processes; and the properties of the media. This study is a two layer problem containing horizontal oil layer overlying the subsurface topsoil region saturated with oil and water (native fluid). To explain the method by which the convective flow in the oil region affect the transportation of oil, modeling is carried out in two regions (oil and topsoil). The two dimensional, transient oil flow equations for both the regions include thermal and concentration buoyancy effects. The species equations include the effects of energy flux caused by the temperature gradient on the unsteady advective-diffusion equation. The resulting fluid flow, heat and mass transfer processes are discussed numerically with the aid of graphs. The validity of the results obtained is verified by comparison with available results and good agreement is found.

1. Introduction

When heat and mass transfer occur simultaneously in a moving fluid, the relations between the fluxes and the driving potentials are of more intricate in nature. It has been observed that mass fluxes can be created by temperature gradients and this embodies the thermal diffusion effect. The thermal diffusion phenomenon, also called Soret effect, occurs in the multicomponent mixture

296

Applications and Applied Mathematics: An International Journal (AAM), Vol. 13 [2018], Iss. 1, Art. 21

AAM: Intern. J., Vol. 13, Issue 1 (June 2018)   297

where temperature gradient induces mass transfer. In most of the studies related to heat and mass transfer processes, Soret effect is neglected on the basis that it is of a smaller order of magnitude than the effects described by FourierÓş and FickÓş laws. But this effect is considered as second order phenomena and may become significant in areas such as hydrology, petrology, geosciences, etc.

Thus the study of thermal diffusion in a fluid saturated porous medium is of importance in geophysics, groundwater hydrology, soil science, oil extraction (Parvathy and Patil, 1989). The reason is that the earth's crust is a porous medium by a mixture of different types of fluids such as oil, water, gases and molten form of ores dissolved in fluids. Thermal gradients present between the interior and exterior of the earth's crust may help convection to set in. The thermal gradient in crude oil can have a strange effect on the distribution of petroleum components in an oil deposit.

Literature review of the thermal diffusion phenomenon shows that several experimental and theoretical studies have been carried out by several authors (Poulikakos, 1986; Chen and Lu, 1992; Carr and Straughan, 2003; Bahadori and Rezvantalab, 2014) on the subject concerned in a system consisting of a horizontal fluid layer over lying a porous medium saturated with that fluid. England et al. (1987) stressed on the chemical and physical properties of petroleum gases and liquids, particularly their phase behavior under subsurface conditions to be important factor in determining petroleum migration behavior. Their study concluded that the directions and magnitudes of the forces acting on migrating petroleum are deduced from the combined effects of buoyancy and water flow in compacting sediments.

Nithiarasu et al. (1998) investigated the effect of porosity on natural convection and heat transfer in a fluid-saturated porous medium using a generalized non-Darcy model with porosity as a separate parameter and applying the Boussinesq approximation to the momentum equation. Shukla and Firoozabadi (1998) presented a model for prediction of the thermal diffusion coefficients in binary fluids using the rules of thermodynamics in irreversible processes. The model was used to predict the coefficients of thermal diffusion at various values of pressure and temperature for hydrocarbon and non-hydrocarbon fluid mixtures.

Finite amplitude convective oscillations in a binary mixture with a Soret effect were theoretically predicted by Shliomis and Souhar (2000). They argued that the concentration gradients sets in slowly in colloidal mixtures with a small particle mobility. Three dimensional numerical modeling of Soret-driven convection in a cubic cell filled with a binary mixture of water and isopropanol was performed by Shevtsova et al. (2006). These authors analyzed the unstable density stratification established in the binary mixture with a negative Soret effect when heated from above.

Mansour et al. (2006) conducted a numerical analysis to study the Soret effect in fluid flow as well as heat and mass transfer due to natural convection in a square porous cavity with a cross concentration and temperature gradients. Md. Rahman and Saghir (2010) investigated the onset of thermo-solutal convection in a liquid layer over a porous layer in a system heated laterally. The study of Melnikov and Shevtsova (2011) analyzed the Soret separation by thermo-diffusion of components of a binary liquid mixture through a porous medium in presence of gravity field. They employed a Darcy-Brinkman model to experimentally model the double-diffusive convection with Soret effect in a system consisting of a fluid region adjacent to a porous medium saturated with

and laterally sandwiched between the same liquid.

A comprehensive review of the literature concerning natural convection in fluid-saturated porous media are detailed by Ingham and Pop (1998, 2005), Nield and Bejan (2006), Vafai (2000, 2005) and Vadasz (2008). Miyan and Pant (2015) analyzed the fluid flow in porous media modeled by postulating a multiphase generalization of the Darcy's law, which is based on the principle of a linear relation between the velocity and the pressure gradient in the porous media. They stated that the multiphase flow is a subject with important technical applications, most notably in oil recovery from petroleum reservoirs and so on.

Motivated by these studies, a mathematical model has been developed to study the movement of oil flow and its characteristics separately in the oil and topsoil region to analyze whether the convective flow of oil in the oil region may affect the transportation of oil in the topsoil region. The model in the present analysis is widened by relating two coupled non-linear partial differential equations dependent on time. We choose this approach, rather than solving the problem in the whole domain, because it is more conductive to explain qualitatively the processes occurring at the permeable fluid-porous interface.

Once spilled oil is released into the subsurface system, oil will interact hydrologically, physically and chemically with both- the native water and the granulated solid matrix. The major hydrological and physical processes of interaction include advection, dispersion, diffusion, decay and chemical reactions. The physical processes determine the way mass is moved from one point to another. The chemical and biological processes redistribute the mass among different chemical forms, or into and out of the system. Thus their mobility and persistence in the topsoil are need to be determined.

The topsoil under study is considered to be homogeneous porous medium bounded by oil formed as a layer on the upper surface. The soil and the fluids(water and oil) are assumed to be incompressible and the flow is transient, two dimensional. The flow equation includes thermal and concentration buoyancy effects in both the oil and topsoil region. The species equation defined for oil particle concentration includes adsorption, degradation and the energy flux caused by temperature gradient. The flow of oil in the topsoil is described by a non-Darcy model with porosity as a separate parameter. The governing equations along with the boundary conditions obtained are simplified using perturbation technique and then solved.

2.   Mathematical Formulation

The considered system in this study consists of the spilled oil moving as a layer and migrating in the topsoil. We use a rectangular coordinate system, (x, y) to model this flow, where, x and y denote the horizontal and vertical coordinates, respectively. The specified geometry under consideration consists of two-layer regions: region I $(h \leq y \leq H)$ is the fluid region containing oil, and region II $(0 \leq y \leq h)$ is the topsoil considered to be a fluid saturated porous medium filled with water(Figure 1). We assume that the topsoil is homogeneous, isotropic and the thermo physical properties such as thermal conductivity, heat capacity, viscosity are considered constant, with the saturated incompressible oil in local thermodynamic equilibrium. Buoyancy forces resulting from the variation of density are taken into account satisfying the linear Boussinesq approximation (Gobin and Goyeau,

Applications and Applied Mathematics: An International Journal (AAM), Vol. 13 [2018], Iss. 1, Art. 21

AAM: Intern. J., Vol. 13, Issue 1 (June 2018) 299

2012):

$\rho = \rho_o \left[1 - \beta_T(T_1 - T_a) - \beta_c(c_1 - c_a)\right]$ in the oil region, and

$\rho = \rho_o \left[1 - \beta_T(T_2 - T_b) - \beta_c(c_2 - c_b)\right]$ in the topsoil region.

For each layer, the mathematical model is developed using the Navier-Stoke's equation, which is one of the most used approach to describe flow in multi-domain system.
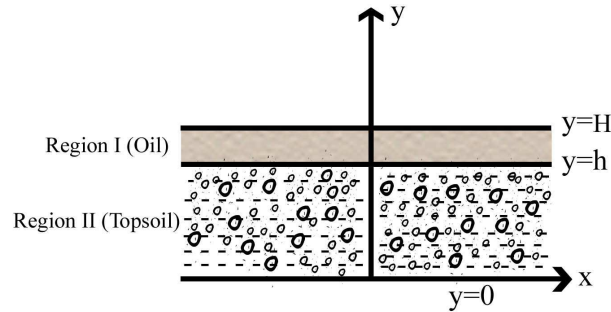

Figure 1. Physical configuration

Region I (Oil)

$$\frac{\partial u_1}{\partial x} + \frac{\partial v_1}{\partial y} = 0, \tag{1}$$

$$\frac{\partial u_1}{\partial t} + u_1 \frac{\partial u_1}{\partial x} + v_1 \frac{\partial u_1}{\partial y} = -\frac{1}{\rho_o}\frac{\partial p_1}{\partial x} + \nu_o \left(\frac{\partial^2 u_1}{\partial x^2} + \frac{\partial^2 u_1}{\partial y^2}\right) + g\beta_T \left(T_1 - T_a\right)$$
$$+ g\beta_c \left(c_1 - c_a\right), \tag{2}$$

$$\frac{\partial v_1}{\partial t} + u_1 \frac{\partial v_1}{\partial x} + v_1 \frac{\partial v_1}{\partial y} = -\frac{1}{\rho_o}\frac{\partial p_1}{\partial y} + \nu_o \left(\frac{\partial^2 v_1}{\partial x^2} + \frac{\partial^2 v_1}{\partial y^2}\right), \tag{3}$$

Region II (Topsoil)

$$\frac{\partial u_2}{\partial x} + \frac{\partial v_2}{\partial y} = 0, \tag{4}$$

$$\frac{\partial u_2}{\partial t} + u_2 \frac{\partial u_2}{\partial x} + v_2 \frac{\partial u_2}{\partial y} = -\frac{1}{\rho_o}\frac{\partial p_2}{\partial x} + \nu_e \varphi \left(\frac{\partial^2 u_2}{\partial x^2} + \frac{\partial^2 u_2}{\partial y^2}\right) + g\varphi\beta_T \left(T_2 - T_b\right)$$
$$+ g\varphi\beta_c \left(c_2 - c_b\right) - \varphi \frac{\nu_o}{k_p} u_2, \tag{5}$$

$$\frac{\partial v_2}{\partial t} + u_2 \frac{\partial v_2}{\partial x} + v_2 \frac{\partial v_2}{\partial y} = -\frac{1}{\rho_o}\frac{\partial p_2}{\partial y} + \nu_e \varphi \left(\frac{\partial^2 v_2}{\partial x^2} + \frac{\partial^2 v_2}{\partial y^2}\right) - \varphi \frac{\nu_o}{k_p} v_2, \tag{6}$$

where (u_1, v_1) and (u_2, v_2) are the velocities of oil in Region I and Region II, along the x and y directions, respectively, t is the time, p_i represents the pressure on Regions I and II for $i = 1, 2$, respectively, T_1 and c_1 are the temperature and concentration of oil in Region I, respectively, T_2 is the temperature distribution of the region II, c_2 is the concentration of oil in water (Region II), φ is the porosity, ρ_o is the density of oil, ν_o is the kinematic viscosity of oil, ν_e is the effective

kinematic viscosity, g is the gravitational acceleration, β_T and β_c are the thermal and concentration expansion coefficients, respectively, k_p is the permeability of the medium and T_a, T_b, c_a and c_b are the constants which define the initial temperature and concentration of the oil and topsoil regions, respectively.

The energy conservation equations for both the regions are:

Region I (Oil)

$$\frac{\partial T_1}{\partial t} + u_1 \frac{\partial T_1}{\partial x} + v_1 \frac{\partial T_1}{\partial y} = \left(\frac{k_T}{\rho c_p} \right)_o \left(\frac{\partial^2 T_1}{\partial x^2} + \frac{\partial^2 T_1}{\partial y^2} \right). \tag{7}$$

In the topsoil, we assume that the energy equation is based on local thermal equilibrium that hypothesizes that the solid and fluid phases are at the same temperature at each point in the medium (Nield and Bejan, 2006). The thermal energy conservation equation for the matrix or solid phase can be expressed as follows:

$$(1 - \varphi)(\rho c_v)_s \frac{\partial T_s}{\partial t} = (1 - \varphi)(k_T)_s \nabla^2 T_s, \tag{8}$$

where, T_s is the temperature of the solid matrix and C_v is the volumetric heat capacity.

For the oil mixture inside the soil, it can be expressed as:

$$(\rho c_p)_o \left[\varphi \frac{\partial T_f}{\partial t} \right] + u.\nabla T_f = \varphi (k_T)_o \nabla^2 T_f, \tag{9}$$

where, T_f is the temperature of the oil mixture. Since the velocity of the matrix is zero, and there is no viscous dissipation and heat generation in either soil or the oil mixture, the thermal equilibrium assumed between the solid and liquid phases occurs very quickly so that $T_s = T_f = T_2$. By adding Equations (8) and (9), the energy conservation equation for topsoil region can be written as follows (Jaber, 2010):

Region II (Topsoil)

$$\sigma_m \frac{\partial T_2}{\partial t} + u_2 \frac{\partial T_2}{\partial x} + v_2 \frac{\partial T_2}{\partial y} = k_m \left(\frac{\partial^2 T_2}{\partial x^2} + \frac{\partial^2 T_2}{\partial y^2} \right), \tag{10}$$

where,

$$\sigma_m = \frac{(1 - \varphi)(\rho c_v)_s + \varphi (\rho c_p)_o}{(\rho c_p)_o},$$

$$k_m = \frac{(1 - \varphi)(k_T)_s + \varphi (K_T)_o}{(\rho c_p)_o},$$

c_p is the specific heat at constant pressure and k_T is the thermal conductivity suffices and s and o refers to solid matrix and oil, respectively.

Here, we have considered the property for the porous region f_{por} as the sum of corresponding values of the solid matrix and of the liquid $f_{por} = (1 - \varphi)f_{solid} + \varphi f_{liq}$. The effective viscosity ν_e is related to the oil viscosity and we model it as: $\nu_e = \nu_{liq}(1 + 2.5(1 - \varphi))$ (Celli Michele, 2010).

Applications and Applied Mathematics: An International Journal (AAM), Vol. 13 [2018], Iss. 1, Art. 21

AAM: Intern. J., Vol. 13, Issue 1 (June 2018)   301

The mass conservation equation in the oil layer and the topsoil which includes:
(i) advection which is caused by flow of oil;
(ii) retardation which is caused by adsorption;
(iii) thermal diffusion caused by temperature gradient; and
(iv) the first-order degradation,
are written as

Region I (Oil)

$$
\frac{\partial c_1}{\partial t} + u_1 \frac{\partial c_1}{\partial x} + v_1 \frac{\partial c_1}{\partial y} = (D_m)_o \left(\frac{\partial^2 c_1}{\partial x^2} + \frac{\partial^2 c_1}{\partial y^2} \right) + \left(\frac{D_m k_T}{T_m} \right)_o \left(\frac{\partial^2 T_1}{\partial x^2} + \frac{\partial^2 T_1}{\partial y^2} \right) \tag{11}
$$
$$
- \mu_c \left(c_1 - c_a \right),
$$

Region II (Topsoil)

$$
\frac{\partial c_2}{\partial t} + \frac{\theta_w}{\theta_o} \frac{\partial c_w}{\partial t} + \frac{\rho_b}{\varphi \theta_o} \frac{\partial q_s}{\partial t} + u_2 \frac{\partial c_2}{\partial x} + v_2 \frac{\partial c_2}{\partial y} = (D_m)_e \left(\frac{\partial^2 c_2}{\partial x^2} + \frac{\partial^2 c_2}{\partial y^2} \right)
$$
$$
+ \frac{(D_m)_e k_m}{T_m} \left(\frac{\partial^2 T_2}{\partial x^2} + \frac{\partial^2 T_2}{\partial y^2} \right) - \mu_c \left(c_2 - c_b \right), \tag{12}
$$

where c_w is the concentration of water in oil, q_s is the weight of oil adsorbed per unit weight of adsorbent (soil), θ_w is the fraction of pore space occupied by water, θ_o is the fraction of pore space occupied by oil, ρ_b is the soil bulk density, $(D_m)_o$ is the mass diffusivity of oil, $(D_m)_e$ is the effective mass diffusivity, T_m is the mean temperature and μ_c is the rate of degradation. The mass diffusion coefficient in the porous region can be different from that in the pure liquid (Takahashi et al., 2002); they are related as $(D_m)_e = \dfrac{(D_m)_o}{\tau^2}$, where, $\tau \geq 1$ is the tortuosity. The tortuosity is not less than unity, hence the diffusion coefficient in porous material is always smaller than in the pure liquid.

Sorption between oil and the soil results in the development of retardation factor. Accounting for equilibrium in linear sorption process, Langmuir model (Dada et al., 2012) describing the adsorption of fluid molecules onto solid adsorbents such as soil defined by $q_s = \dfrac{q \, k_{s-o} \, c_2}{1 + k_{s-o} c_2}$ simplifies the retardation factor $R = 1 + \frac{\theta_w}{\theta_o} k_{w-o} + \dfrac{\rho_b}{\varphi \theta_o} q k_{s-o}$, where q is the maximum adsorption capacity of the soil, $k_{w-o}, \, k_{s-o}$ are adsorption coefficients (partition coefficient between water and oil, soil solids and oil, respectively) and $c_w = k_{w-o} c_2$, reduces Equation (12) to

$$
R \frac{\partial c_2}{\partial t} + u_2 \frac{\partial c_2}{\partial x} + v_2 \frac{\partial c_2}{\partial y} = (D_m)_e \left(\frac{\partial^2 c_2}{\partial x^2} + \frac{\partial^2 c_2}{\partial y^2} \right) + \frac{(D_m)_e k_m}{T_m} \left(\frac{\partial^2 T_2}{\partial x^2} + \frac{\partial^2 T_2}{\partial y^2} \right) \tag{13}
$$
$$
- \mu_c \left(c_2 - c_b \right).
$$

In order to obtain a well-posed problem, the initial and boundary conditions must be formulated in an appropriate manner. As the interface region between the oil and the topsoil was permeable to allow the oil to move between layers, the porous/fluid interface boundary conditions has been

imposed for velocity and temperature (Beavers and Joseph, 1967; Huang and Vafai, 1993). The appropriate conditions are:

Initial conditions:

$$\left.\begin{array}{l} u_1 = 0 \ , \ v_1 = 0 \ , \ T_1 = T_a \ , \ c_1 = c_a \ at \ h \ < \ y \ < \ H, \ t \leq 0 \ ; \\ u_2 = 0 \ , \ v_2 = 0 \ , \ T_2 = T_b \ , \ c_2 = c_b \ at \ 0 \ < \ y \ < \ h, \ t \leq 0. \end{array}\right\} \tag{14}$$

Boundary conditions:

$$\left.\begin{array}{l} u_1 = v_0(1 + \epsilon e^{\mathbf{i}(\alpha x + \omega t)}), \ v_1 = 0, \ T_1 = T_a, \ c_1 = c_a \ \ at \ y = H \ , \ t > 0 \ ; \\[2mm] \dfrac{\partial u_2}{\partial y} = \dfrac{\alpha_p}{\sqrt{k_p}}(u_2 - u_1) \ , \ p_1 = p_2 \ , \mu_o\left(\dfrac{\partial u_1}{\partial y} + \dfrac{\partial v_1}{\partial x}\right) = \dfrac{\mu_e}{\varphi}\left(\dfrac{\partial u_2}{\partial y} + \dfrac{\partial v_2}{\partial x}\right) \ , \\[2mm] v_1 = v_2 \ , \ T_1 = T_2 \ , \ \dfrac{\partial T_2}{\partial y} = \dfrac{(k_T)_o}{(k_T)_s}\dfrac{\partial T_1}{\partial y} \ , \ c_1 = c_a + c_{10}e^{-\mu_c t}(1 + \epsilon e^{\mathbf{i}(\alpha x + \omega t)}) \ , \\[2mm] c_2 = c_b + c_{20}e^{-\mu_c t}(1 + \epsilon e^{\mathbf{i}(\alpha x + \omega t)}) \ at \ y = h, \ t > 0 \ ; \\[2mm] u_2 = 0 \ , \ v_2 = 0, \ T_2 = T_0, \ c_2 = c_0 \ at \ y = 0, \ t > 0, \end{array}\right\} \tag{15}$$

where α_p is the slip parameter, α is the stream-wise wave number with its dimension as inverse of space variable x, ω is the frequency parameter with its dimension as inverse of time t, $c_{10}, \ c_{20}, \ T_0$ and c_0 are constants, ϵ is the perturbation parameter and $\mathbf{i}$ represents the imaginary part.

The non-dimensional quantities which transform the governing equations and conditions into dimensionless form are:

$$(x^*, y^*) = \frac{v_0}{\nu_o}(x, y), \quad t^* = \frac{tv_0^2}{\nu_o}, \quad (u_i^*, v_i^*) = \frac{1}{v_0}(u_i, v_i), \quad p_i^* = \frac{p_i}{\rho_o v_0^2}, \quad (i = 1, 2)$$

$$T_1^* = \frac{T_1 - T_a}{\Delta T_1}, \quad C_1^* = \frac{c_1 - c_a}{\Delta c_1}, \quad T_2^* = \frac{T_2 - T_b}{\Delta T_2}, \quad C_2^* = \frac{c_2 - c_b}{\Delta c_2},$$

where the temperature and concentration differences are scaled by $\Delta T_1 = T_0 - T_a \ , \ \Delta T_2 = T_0 - T_b \ , \ \Delta c_1 = c_0 - c_a \ , \Delta c_2 = c_0 - c_b$ and v_0 is the characteristic velocity.

Neglecting the '*' symbol, the dimensionless form of Equations (1) to (7), (10), (11) and (13) take the form

Region I

$$\frac{\partial u_1}{\partial x} + \frac{\partial v_1}{\partial y} = 0, \tag{16}$$

$$\frac{\partial u_1}{\partial t} + u_1\frac{\partial u_1}{\partial x} + v_1\frac{\partial u_1}{\partial y} = -\frac{\partial p_1}{\partial x} + \frac{\partial^2 u_1}{\partial x^2} + \frac{\partial^2 u_1}{\partial y^2} + Gr_1 T_1 + Gc_1 \, C_1, \tag{17}$$

Applications and Applied Mathematics: An International Journal (AAM), Vol. 13 [2018], Iss. 1, Art. 21

AAM: Intern. J., Vol. 13, Issue 1 (June 2018) 303

$$\frac{\partial v_1}{\partial t} + u_1 \frac{\partial v_1}{\partial x} + v_1 \frac{\partial v_1}{\partial y} = -\frac{\partial p_1}{\partial y} + \frac{\partial^2 v_1}{\partial x^2} + \frac{\partial^2 v_1}{\partial y^2}, \tag{18}$$

$$\frac{\partial T_1}{\partial t} + u_1 \frac{\partial T_1}{\partial x} + v_1 \frac{\partial T_1}{\partial y} = \frac{1}{Pr_o} \left(\frac{\partial^2 T_1}{\partial x^2} + \frac{\partial^2 T_1}{\partial y^2} \right), \tag{19}$$

$$\frac{\partial C_1}{\partial t} + u_1 \frac{\partial C_1}{\partial x} + v_1 \frac{\partial C_1}{\partial y} = \frac{1}{Sc_o} \left(\frac{\partial^2 C_1}{\partial x^2} + \frac{\partial^2 C_1}{\partial y^2} \right) + So_o \left(\frac{\partial^2 T_1}{\partial x^2} + \frac{\partial^2 T_1}{\partial y^2} \right) - \mu_d C_1, \tag{20}$$

Region II

$$\frac{\partial u_2}{\partial x} + \frac{\partial v_2}{\partial y} = 0, \tag{21}$$

$$\begin{aligned}
\frac{\partial u_2}{\partial t} + u_2 \frac{\partial u_2}{\partial x} + v_2 \frac{\partial u_2}{\partial y} = &- \frac{\partial p_2}{\partial x} + \varphi R_\nu \left(\frac{\partial^2 u_2}{\partial x^2} + \frac{\partial^2 u_2}{\partial y^2} \right) + \varphi Gr_2 T_2 \\
&+ \varphi Gc_2 \, C_2 - \varphi \sigma^2 u_2,
\end{aligned} \tag{22}$$

$$\frac{\partial v_2}{\partial t} + u_2 \frac{\partial v_2}{\partial x} + v_2 \frac{\partial v_2}{\partial y} = -\frac{\partial p_2}{\partial y} + \varphi R_\nu \left(\frac{\partial^2 v_2}{\partial x^2} + \frac{\partial^2 v_2}{\partial y^2} \right) - \varphi \sigma^2 v_2, \tag{23}$$

$$\sigma_m \frac{\partial T_2}{\partial t} + u_2 \frac{\partial T_2}{\partial x} + v_2 \frac{\partial T_2}{\partial y} = \frac{1}{Pr_e} \left(\frac{\partial^2 T_2}{\partial x^2} + \frac{\partial^2 T_2}{\partial y^2} \right), \tag{24}$$

$$R \frac{\partial C_2}{\partial t} + u_2 \frac{\partial C_2}{\partial x} + v_2 \frac{\partial C_2}{\partial y} = \frac{1}{Sc_e} \left(\frac{\partial^2 C}{\partial x^2} + \frac{\partial^2 C_2}{\partial y^2} \right) + So_e \left(\frac{\partial^2 T_2}{\partial x^2} + \frac{\partial^2 T_2}{\partial y^2} \right) - \mu_d C_2, \tag{25}$$

where,

$\sigma = \dfrac{\nu_o}{v_0 \sqrt{k_p}}$ is the porous parameter,

$R_\nu = \dfrac{\nu_e}{\nu_o}$ is the kinematic viscosity ratio,

$\mu_d = \dfrac{\mu_c \nu_o}{v_0^2}$ is the dimensionless degradation rate parameter,

$Gr_i = \dfrac{\nu_o g \beta_T (\Delta T_i)}{v_0^3}$ is the thermal Grashof number in the oil and topsoil region, respectively for $i = 1, 2$,

$Gc_i = \dfrac{\nu_o g \beta_c (\Delta c_i)}{v_0^3}$ is the mass Grashof number in the oil and topsoil region, respectively for $i = 1, 2$,

$Pr_o = \left(\dfrac{\rho c_p \nu}{k_T} \right)_o$ is the Prandtl number in the oil region,

$Pr_e = \dfrac{\nu_o}{k_m}$ is the effective Prandtl number in the topsoil region,

$Sc_o = \dfrac{\nu_o}{(D_m)_o}$ is the Schmidt number in the oil region,

$Sc_e = \dfrac{\nu_o}{D_{m\,e}}$ is the effective Schmidt number in the topsoil region,

$So_o = \left(\dfrac{D_m k_T}{T_m \nu} \right)_o \dfrac{\Delta T_1}{\Delta c_1}$ is the Soret number in the oil region and,

$So_e = \dfrac{(D_m)_e k_m}{T_m \nu_o} \dfrac{\Delta T_2}{\Delta c_2}$ is the effective Soret number in the topsoil region.

The initial and boundary conditions (14) and (15) in non-dimensional form are:

$$\left. \begin{array}{l} u_1 = 0 \,, \; v_1 = 0 \,, \; T_1 = 0 \,, \; C_1 = 0 \; at \; h \; < \; y \; < \; H, \; t \leq 0 \,; \\[4pt] u_2 = 0 \,, \; v_2 = 0 \,, \; T_2 = 0 \,, \; C_1 = 0 \; at \; 0 \; < \; y \; < \; h, \; t \leq 0 \end{array} \right\} \tag{26}$$

and

$$\left. \begin{array}{c} u_1 = 1 + \epsilon e^{\mathbf{i}(\alpha x + \omega t)}, \; v_1 = 0, \; T_1 = 0, \; C_1 = 0 \; at \; y = H \,, \; t > 0 \,; \\[10pt] \dfrac{\partial u_2}{\partial y} = \alpha_p \sigma (u_2 - u_1) \,, \; p_1 = p_2 \,, \; \dfrac{\partial u_1}{\partial y} + \dfrac{\partial v_1}{\partial x} = \dfrac{R_\mu}{\varphi} \left(\dfrac{\partial u_2}{\partial y} + \dfrac{\partial v_2}{\partial x} \right) \,, \\[10pt] v_1 = v_2 \,, \; T_1 = T_2 \,, \; \dfrac{\partial T_1}{\partial y} = R_{k_T} \dfrac{\partial T_2}{\partial y} \,, \; C_1 = c_{a_o} e^{-\mu_d t}(1 + \epsilon e^{\mathbf{i}(\alpha x + \omega t)}) \,, \\[10pt] C_2 = c_{b_o} e^{-\mu_d t}(1 + \epsilon e^{\mathbf{i}(\alpha x + \omega t)}) \; at \; y = h, \; t > 0 \,; \\[10pt] u_2 = 0 \,, \; v_2 = 0, \; T_2 = 1, \; C_2 = 1 \; at \; y = 0, \; t > 0, \end{array} \right\} \tag{27}$$

where,

$R_\mu = \dfrac{\mu_e}{\mu_o}$ is the dynamic viscosity ratio,

$R_{k_T} = \dfrac{(k_T)_s}{(k_T)_o}$ is the thermal conductivity ratio,

c_{a_o} and c_{b_o} are constants.

3. Method of Solution

We decompose the flow, thermal and the concentration variables into steady base state quantities (designated by upper-case letters) and two-dimensional linear perturbations (designated by a hat) as

$$(u_i, v_i, p_i, T_i, C_i) = (U_{B_i}(y), 0, P_{B_i}(x), T_{B_i}(y), C_{B_i}(y))$$
$$+ (\hat{u}_i, \hat{v}_i, \hat{p}_i, \hat{T}_i, \hat{c}_i)(y) \, \epsilon \, e^{\mathbf{i}(\alpha x + \omega t)} + o(\epsilon^2), \tag{28}$$

for $i = 1, 2$. Substituting (28) into Equations (16) to (25) and the boundary conditions (27), neglecting the higher order of (ϵ^2) and equating the zeroth and first order terms we obtain the following set of ordinary differential equations and their boundary conditions.

3.1. Base State

By assuming a steady, parallel, fully developed flow, the base state equations obtained are:

$$\frac{d^2 U_{B_1}}{dy^2} = \frac{dP_{B_1}}{dx} - Gr_1 T_{B_1} - Gc_1 C_{B_1}, \tag{29}$$

$$\frac{d^2 U_{B_2}}{dy^2} - \frac{\sigma^2}{R_\nu} U_{B_2} = \frac{1}{R_\nu} \left(\varphi \frac{dP_{B_2}}{dx} - Gr_2 T_{B_2} - Gc_2 C_{B_2} \right), \tag{30}$$

$$\frac{d^2 T_{B_1}}{dy^2} = 0, \tag{31}$$

$$\frac{d^2 T_{B_2}}{dy^2} = 0, \tag{32}$$

$$\frac{d^2 C_{B_1}}{dy^2} - \mu_d Sc_o C_{B_1} = 0, \tag{33}$$

$$\frac{d^2 C_{B_2}}{dy^2} - \mu_d Sc_e C_{B_2} = 0, \tag{34}$$

subject to the boundary conditions,

$$U_{B_1} = 1, \ T_{B_1} = 0, \ C_{B_1} = 0 \ at \ y = H \ ;$$

$$\frac{dU_{B_2}}{dy} = \alpha_p \sigma (U_{B_2} - U_{B_1}) \ , \ P_{B_1} = P_{B_2} \ , \ \frac{dU_{B_1}}{dy} = \frac{R_\mu}{\varphi} \frac{dU_{B_2}}{dy} \ ,$$

$$T_{B_1} = T_{B_2} \ , \ \frac{dT_{B_1}}{dy} = R_{k_T} \frac{dT_{B_2}}{dy} \ , \tag{35}$$

$$C_{B_1} = c_{a_O} e^{-\mu_d t} \ , \ C_{B_2} = c_{b_O} e^{-\mu_d t} \ at \ y = h \ ;$$

$$U_{B_2} = 0 \ , \ T_{B_2} = 1 \ , \ C_{B_2} = 1 \ at \ y = 0.$$

Solving the above Equations (29) to (34), the base state velocities, temperature and concentration using the boundary conditions (35) are

$$U_{B_1} = \frac{g_3 y^2}{2} - \frac{Gr_1 g_6 R_{K_T}}{6}(y^3 - 3Hy^2) - \frac{Gc_1 g_7}{g_1}\left(e^{\sqrt{g_1}\,y} - e^{2\sqrt{g_1}\,H}e^{-\sqrt{g_1}\,y}\right)$$
$$+ g_{11}(y - H) + \left(1 - \frac{g_3 H^2}{2} - \frac{Gr_1 g_6 R_{K_T} H^3}{3}\right), \tag{36}$$

$$U_{B_2} = g_{14}(e^{\sqrt{g_5}\,y} - e^{-\sqrt{g_5}\,y}) + \left(\frac{g_4}{g_5} - \frac{Gr_2}{R_\nu g_5} + \frac{Gc_2}{R_\nu(g_2 - g_5)}\right)e^{-\sqrt{g_5}\,y} - \frac{g_4}{g_5}$$
$$+ \frac{Gr_2(g_6 y + 1)}{R_\nu g_5} - \frac{Gc_2(g_8 e^{\sqrt{g_2}\,y} + (1 - g_8)\,e^{-\sqrt{g_2}\,y})}{R_\nu(g_2 - g_5)}, \tag{37}$$

$$T_{B_1} = R_{k_T} g_6(y - H) \tag{38}$$

$$T_{B_2} = g_6 y + 1, \tag{39}$$

$$C_{B_1} = g_7\left(e^{\sqrt{g_1}\,y} - e^{2\sqrt{g_1}\,H}e^{-\sqrt{g_1}\,y}\right), \tag{40}$$

$$C_{B_2} = g_8 e^{\sqrt{g_2}\,y} + (1 - g_8)\,e^{-\sqrt{g_2}\,y}, \tag{41}$$

where the constants g_i for $i = 1\,to\,14$ are given in the Appendix.

Assuming uniform pressure$(p_1 = p_2)$ in both the regions, the dimensionless pressure gradient is determined numerically satisfying the condition $\int_0^h U_{B_2} dy + \int_h^H U_{B_1} dy = 1$.

3.2.   Perturbed Part

The stream function is a useful mathematical model that is used to solve the continuity and momentum equations directly for a single variable. Restricting our attention to the real parts of the solutions for the perturbed quantities, re-expressing them in terms of the stream-function $(\hat{u}_i, \hat{v}_i) = (\hat{\phi}_{iy}, -\hat{\phi}_{ix})(i = 1, 2)$ and eliminating the pressure perturbations yields the following set of equations(after suppressing hat (ˆ) symbols):

$$\phi_1^{''''} + \left[(\omega + \alpha U_{B_1})\tan(\alpha x + \omega t) + \alpha^2 \tan^2(\alpha x + \omega t) - \alpha^2\right]\phi_1^{''}$$
$$+ \left[\alpha^2(\omega + \alpha U_{B_1})\tan^3(\alpha x + \omega t) - \alpha^4 \tan^2(\alpha x + \omega t) - \alpha \tan(\alpha x + \omega t)U_{B_1}^{''}\right]\phi_1 \tag{42}$$
$$+ Gr_1 T_1' + Gc_1 c_1' = 0,$$

$$\phi_2^{''''} + \left[\frac{1}{\varphi R_\nu}(\omega + \alpha U_{B_2})\tan(\alpha x + \omega t) + \alpha^2 \tan^2(\alpha x + \omega t) - \frac{\sigma^2}{R_\nu} - \alpha^2\right]\phi_2^{''}$$
$$+ \left[\left(\varphi R_\nu(\omega + \alpha U_{B_2})\tan(\alpha x + \omega t) - \frac{\sigma^2}{R_\nu} - \alpha^2\right)\alpha^2 \tan^2(\alpha x + \omega t)\right. \tag{43}$$
$$\left. - \frac{1}{\varphi R_\nu}\alpha \tan(\alpha x + \omega t)U_{B_2}^{''}\right]\phi_2 + \frac{Gr_2}{R_\nu}T_2' + \frac{Gc_2}{R_\nu}c_2' = 0,$$

$$T_1'' + \left[Pr_o \left(\omega + \alpha U_{B_1} \right) \tan(\alpha x + \omega t) - \alpha^2 \right] T_1 = Pr_o \, \alpha \tan(\alpha x + \omega t) T_{B_1}' \phi_1, \tag{44}$$

$$T_2'' + \left[Pr_e \left(\omega \sigma_m + \alpha U_{B_2} \right) \tan(\alpha x + \omega t) - \alpha^2 \right] T_2 = Pr_e \, \alpha \tan(\alpha x + \omega t) T_{B_2}' \phi_2, \tag{45}$$

$$c_1'' + \left[Sc_o \left(\omega + \alpha U_{B_1} \right) \tan(\alpha x + \omega t) - \mu_d Sc_o - \alpha^2 \right] c_1 = Sc_o \, \alpha \tan(\alpha x + \omega t) C_{B_1}' \phi_1$$
$$- Sc_o \, So_o \left(T_1'' - \alpha^2 T_1 \right), \tag{46}$$

$$c_2'' + \left[Sc_e \left(\omega R + \alpha U_{B_2} \right) \tan(\alpha x + \omega t) - \mu_d Sc_e - \alpha^2 \right] c_2 = Sc_e \, \alpha \tan(\alpha x + \omega t) C_{B_2}' \phi_2$$
$$- Sc_e \, So_e \left(T_2'' - \alpha^2 T_2 \right), \tag{47}$$

where the prime ($'$) denotes differentiation with respect to y.

The above Equations (42) to (47) are solved numerically subject to the boundary conditions outlined below using *Mathematica 8.0*.

$$\phi_1' = 1, \ \phi_1 = 0, \ T_1 = 0, \ c_1 = 0 \ at \ y = H \ ;$$

$$\phi_2'' = \alpha_p \sigma(\phi_2' - \phi_1'), \ \phi_1'' - \alpha^2 \tan^2(\alpha x + \omega t)\phi_1 = \frac{R_\mu}{\varphi} \left(\phi_2'' - \alpha^2 \tan^2(\alpha x + \omega t)\phi_2 \right),$$

$$\phi_1 = \phi_2, \ \phi_1''' + \left[(\omega + \alpha U_{B_1}) \tan(\alpha x + \omega t) - \alpha^2 \right] \phi_1' - \alpha \tan(\alpha x + \omega t)U_{B_1}' \phi_1$$

$$+ Gr_1 T_1 + Gc_1 c_1 = \varphi R_\nu \left[\phi_2''' + \left(\frac{1}{\varphi R_\nu} (\omega + \alpha U_{B_2}) \tan(\alpha x + \omega t) - \frac{\sigma^2}{R_\nu} - \alpha^2 \right) \phi_2' \right.$$

$$\left. - \alpha \tan(\alpha x + \omega t)U_{B_2}' \phi_2 + \frac{Gr_2}{R_\nu} T_2 + \frac{Gc_2}{R_\nu} c_2 \right],$$

$$T_1 = T_2, \ T_1' = R_{k_T} T_2', \ c_1 = c_{a_0} e^{-\mu_d t}, \ c_2 = c_{b_0} e^{-\mu_d t} \ at \ y = h \ ;$$

$$\phi_2' = 0, \ \phi_2 = 0, \ T_2 = 0, \ c_2 = 0 \ at \ y = 0.$$

(48)

Differentiating the solutions of ϕ_1 and ϕ_2 with respect to y gives the perturbed axial velocity, u_1 and u_2 of oil on the oil and topsoil region, respectively. The base part solutions given by Equations (36) to (41) along with the obtained numerical solutions gives the velocity, temperature and concentration distributions on both the regions.

4. Results and Discussion

Some numerical calculations have been carried out for the non-dimensional velocity, temperature and concentration distributions for the flow under consideration and their behavior have been discussed in both the oil (Region I) and topsoil (Region II) regions for variations in the governing parameters such as thermal and mass Grashof number, porosity, Prandtl number and Soret number. The values of other physical parameters are fixed as real constants (Melnikov and Shevtsova, 2011).
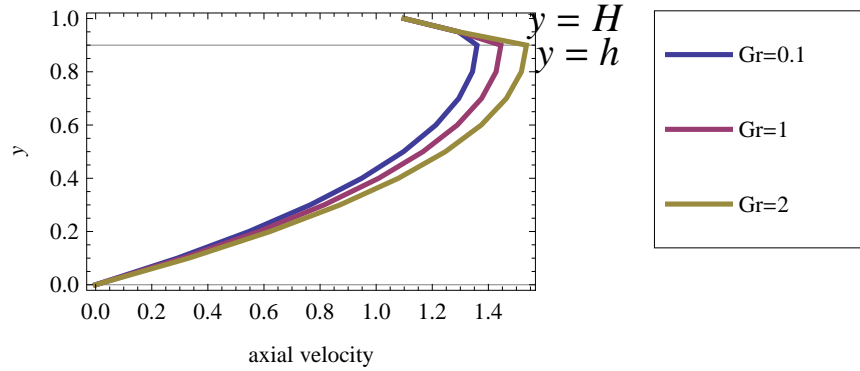
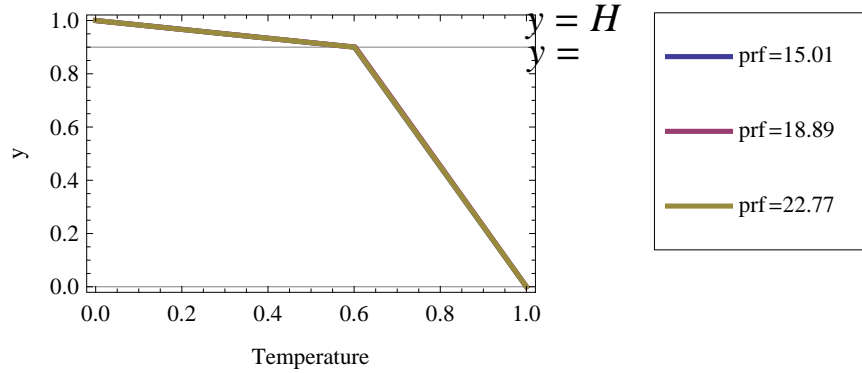**Figure 2.** Effect of thermal Grashof on axial velocity in both the oil and topsoil regions
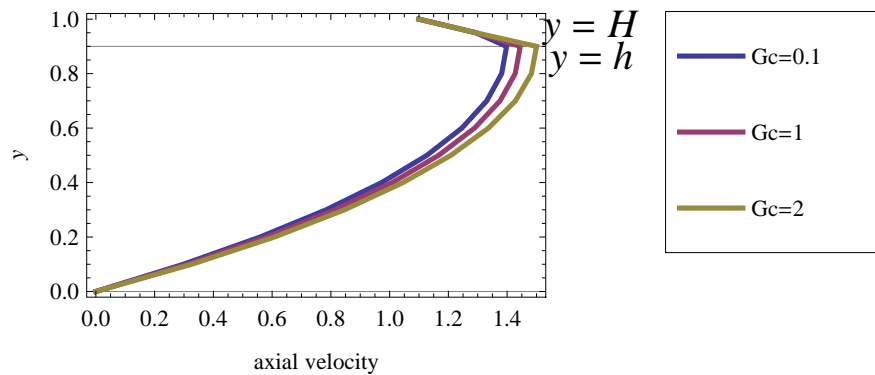
Figure 3. Effect of mass Grashof number on axial velocity in both the oil and topsoil regions
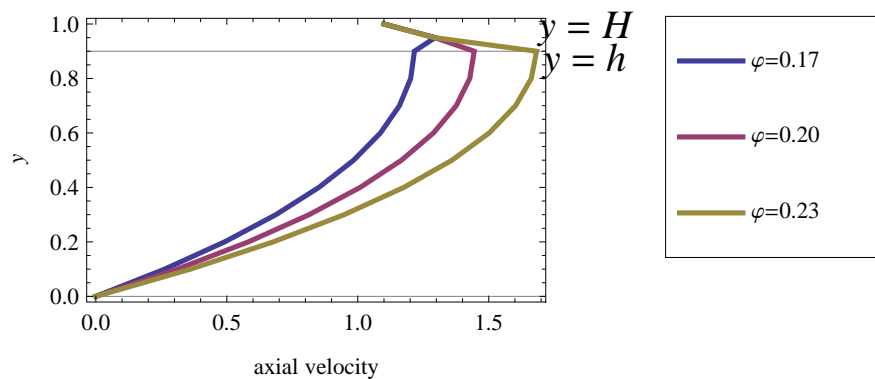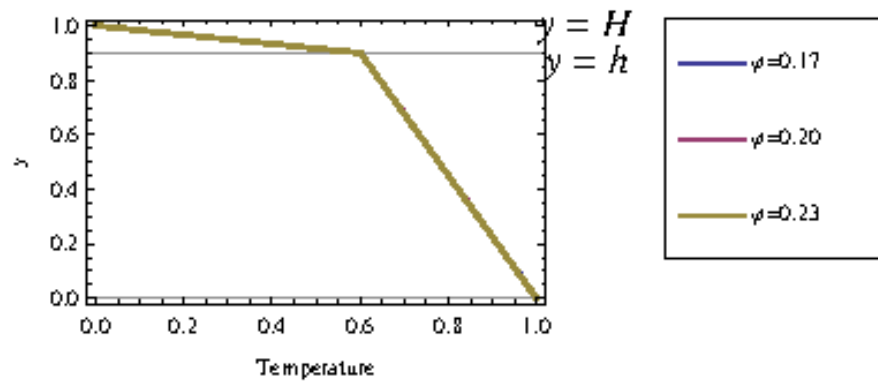

**Figure 4.** Effect of porosity on axial velocity in both the oil and topsoil regions

The axial velocity profile for different thermal and mass Grashof numbers, porosity values in both the oil and topsoil regions are exhibited in Figures 2, 3 and 4, respectively. Natural convection effect is presented in terms of the thermal and mass Grashof numbers. From Figures 2 and 3, we observe that increasing these parameter values enhances velocity profile. This is due to the advancement in the buoyancy ratio that tends to accelerate the fluid flow. Porosity, also known as the void fraction, is the measure of the empty space in a material defined by the ratio of the volume of voids to the

Applications and Applied Mathematics: An International Journal (AAM), Vol. 13 [2018], Iss. 1, Art. 21

AAM: Intern. J., Vol. 13, Issue 1 (June 2018)   309

Figure 5. Effect of Prandtl number on temperature distribution in both the oil and topsoil regions
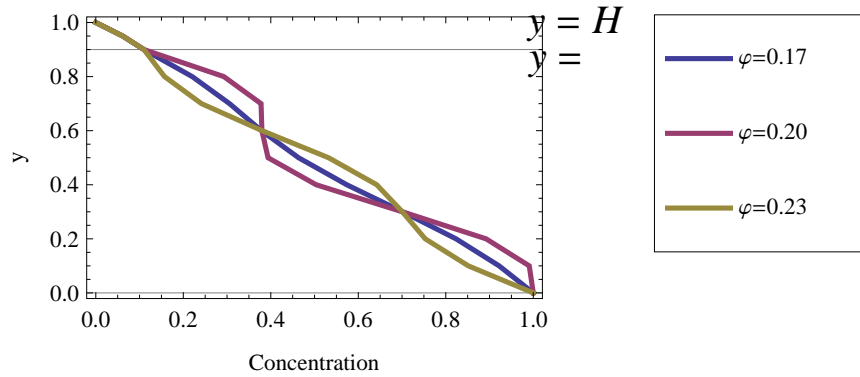

Figure 6. Effect of porosity on temperature distribution in both the oil and topsoil regions
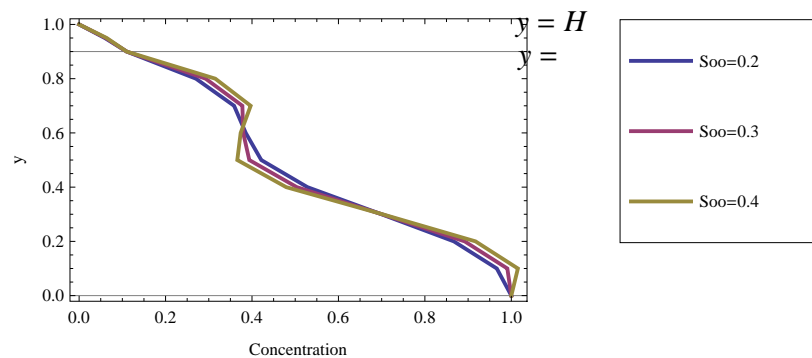

Figure 7. Effect of Soret number on concentration distribution in both the oil and topsoil regions

total volume. Figure 4 depicts that the velocity magnitudes are larger for higher porosity values in the topsoil.

Figures 2, 3 and 4 show that the velocity variations are very small in the oil region. Also, we see that the velocity of oil decreases with depth in the topsoil. This agrees with the similar results of Miyan and Pant (2015) which states that NAPL contaminants such as hydrocarbons travel at a speed that continually decreases with depth and time rather than traveling at a constant speed in the

Figure 8. Effect of porosity on concentration distribution in both the oil and topsoil regions
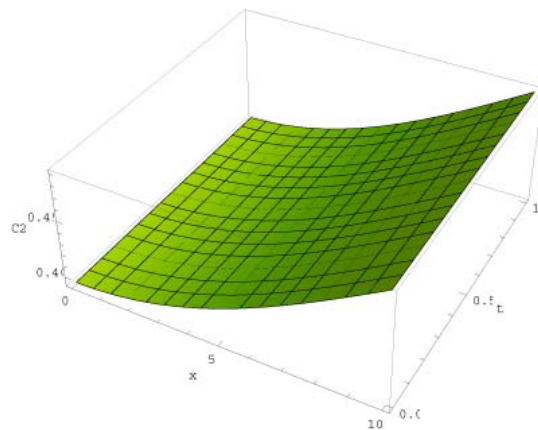
Figure 9. Spatio-temporal (x, t) evolution for the concentration distribution in the topsoil region
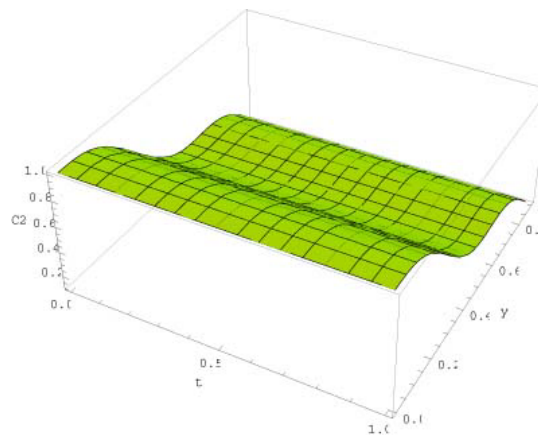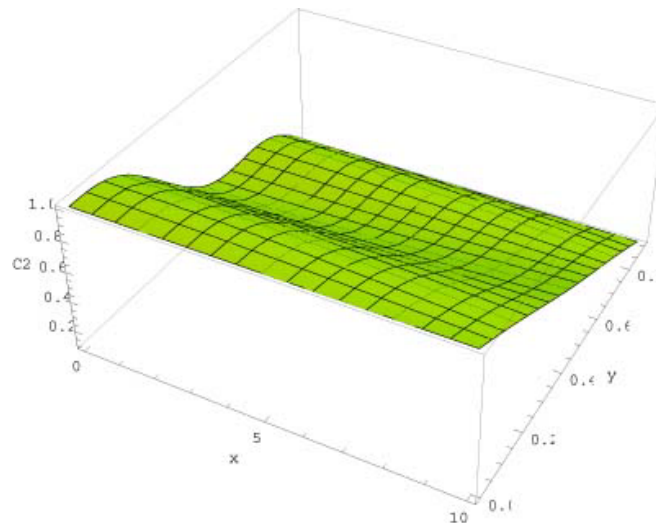

Figure 10. Temporal evolution for the concentration distribution in the topsoil region along depth height

subsurface. They applied Darcy's equation whereas our analysis includes two phase flow, related to two coupled non-linear partial differential equations dependent on time.

Figure 5 show the numerical result of Prandtl number on the dimensionless temperature profile in both the oil and topsoil regions. Here, we see that the temperature increases along the depth of the

Figure 11. Spacial evolution for the concentration distribution in the topsoil region

topsoil and obviously the figure shows neglecting effect on varying Prandtl number values. As the convection in porous media is at least thousand times weaker and the mass transport is controlled by diffusion the effect of porosity is very smaller but not negligible in heat transfer. This can be viewed from Figure 6 which represents the temperature distribution for different porosity values.

The concentration distribution of oil for different Soret numbers and porosity values in both the oil and topsoil regions are discussed through Figures 7 and 8, respectively. These figures show that the concentration of oil increases with the depth of soil, in general.

Figure 7 depicts the concentration distribution of oil for different Soret numbers. From this figure, it is noticed that the fluctuations raises with increasing Soret number values. It is found that the Soret effect affect the heat and mass transfer in the subsurface topsoil region in small variations, and it can improve or impair the mass transfer, depending on the flow structure. As a result of the buoyant convection, the concentration field in pure oil region is uniform creating pronounced boundary layers at the border.

Figure 8 display the effect of porosity on concentration distribution. The fluctuations in the curve shows the presence of trigonometric function existing in the solution.

The temporal and spatial evolution of concentration of oil in the topsoil region (C_2) are depicted in Figures 9, 10 and 11. The migration of oil together with its vapor and dissolved components through the topsoil is a highly complex combination of processes which occur at different spatial and temporal scales. This plot is used to explore the potential relationship between the predictor variables $(x,\ y$ and $t)$ and the response variable (C_2). Figure 9 represents the temporal evolution of concentration of oil along the axial distance. Here we observe that the streamwise coordinate enhances the concentration distribution with increasing time. Figures 10 and 11 pictures the concentration distribution for depth height with respect to time and axial distance. It is found that the concentration increases with increasing depth of the topsoil with respect to time t and the axial distance x, respectively. The waviness in the surface plots involved indicates the periodic fluctuations.

5.   Conclusion

The analysis of the obtained results shows that the velocity of oil decreases with depth in the topsoil due to the block of oil in soil pores. This agrees with the results of Miyan and Pant (2015) which states that NAPL contaminants such as hydrocarbons travel at a speed that continually decreases with depth and time rather than traveling at a constant speed in the subsurface. It is also observed that the concentration of oil increases along the depth of the topsoil and decreases monotonously with increasing time. It is found that the Soret effect affect the heat and mass transfer in both regions with small variations and it can improve or impair the mass transfer depending on the flow structure.

REFERENCES

Bahadori, F. and Rezvantalab, S. (2014). Effects of temperature and concentration dependent viscosity on onset of convection in porous media, Journal of Chemical Technology and Metallurgy, Vol. 49, No. 6, pp. 541–544.

Beavers, G. S., and Joseph, D. D. (1967). Boundary condition at a naturally permeable wall, Journal of Fluid Mechanics, Vol. 30, pp. 197–207.

Carr, M. and Straughan, B. (2003). Penetrative convection in a fluid overlying a porous layer, Advances in Water Resources, Vol. 26, No. 3, pp. 263–276.

Celli Michele. (2010). *Stability, viscous dissipation and local thermal non-equilibrium in fluid saturated porous media*, Ph.D. Thesis, University of Bologna.

Chen, F. and Lu, J. W. (1992). Variable viscosity effects on convective instability in superposed fluid and porous layers, Physics of Fluids A: Fluid Dynamics, Vol. 4, No. 9, pp. 1936–1944.

Dada, A. O., Olalekan, A. P., Olatunya, A. M., and Dada, O. (2012). Langmuir, Freundlich, Temkin and Dubinin-Radushkevich isotherms studies of equilibrium sorption of Zn^{2+} unto phosphoric acid modified rice husk, IOSR Journal of Applied Chemistry, Vol. 3, No. 1, pp. 38–45.

England, W. A., Mackenzie, A. S., Mann, D. M. and Quigley, T. M. (1987). The movement and entrapment of petroleum fluids in the subsurface, Journal of the Geological Society, Vol. 144, No. 2, pp. 327–347.

Gobin, D., and Goyeau, B. (2012). Thermosolutal natural convection in partially porous domains, Journal of Heat Transfer, Vol. 134, No. 3, 031013 (10 pages).

Huang, P. C. and Vafai, K. (1993). Flow and heat transfer control over an external surface using a porous block array arrangement, International Journal of Heat and Mass Transfer, Vol. 36, No. 16, pp. 4019–4032.

Ingham, D. B. and Pop, I. (1998). *Transport Phenomena in Porous Media*, Pergamon, Oxford.

Applications and Applied Mathematics: An International Journal (AAM), Vol. 13 [2018], Iss. 1, Art. 21

AAM: Intern. J., Vol. 13, Issue 1 (June 2018)   313

Ingham, D. B. and Pop, I. (2005). *Transport Phenomena in Porous Media*, Vol. 3, Elsevier, Oxford.

Jaber, T.J. (2010). *Theoretical and experimental investigation of thermodiffusion (Soret effect) in a porous medium*, Ph.D. Thesis, Ryerson University.

Mansour, A., Amahmid, A., Hasnaoui, M. and Bourich, M. (2006). Multiplicity of solutions induced by thermosolutal convection in a square porous cavity heated from below and submitted to horizontal concentration gradient in the presence of Soret effect, Numerical Heat, Transfer Part A, Vol. 49, pp. 69–94.

Rahman, M. A. and Saghir, M. Z. (2010). Thermo-solutal convection in water-isopropanol mixtures in the presence of Soret effect, International Journal of Fluid Mechanics Research, Vol. 37, No. 3, pp. 237–250.

Melnikov, D. E. and Shevtsova, V. M. (2011). Separation of a binary liquid mixture in compound system: Fluid-porous-fluid, Acta Astronautica, Vol. 69, pp. 381–386.

Miyan, M. and Pant, P. K. (2015). Flow and diffusion equations for fluid flow in porous rocks for the multiphase flow phenomena, American Journal of Engineering Research, Vol. 4, No. 7, pp. 139-148.

Nield, D. A. and Bejan, A. (2006). *Convection in Porous Media*, Springer, 3rd edition.

Nithiarasu, P., Seetharamu, K. N., and Sundararajan, T. (1998). Effect of porosity on natural convective heat transfer in a fluid saturated porous medium, International Journal of Heat and Fluid Flow, Vol. 19, No. 1, pp. 56–58.

Parvathy, C. P. and Patil, P. R. (1989). Effect of thermal diffusion on thermohaline interleaving in a porous medium due to horizontal gradients, Indian J. Pure Appl. Math., Vol. 20, No. 7, pp. 716-727.

Poulikakos, D. (1986). Buoyancy driven convection in a horizontal fluid layer extending over a porous substrate, Physics of Fluids, Vol. 29, No. 12, pp. 3949–3957.

Shevtsova, V. M., Melnikov, D. E. and Legros, J. C. (2006). Onset of convection in Soret driven instability, Physical Review E, Vol. 73, 047302 (4 pages).

Shliomis, M. I. and Souhar, M. (2000). Self-oscillatory convection caused by the Soret effect, Europhysics Letters, Vol. 49, No. 1, pp. 55–61.

Shukla, K., and Firoozabadi, K. A. (1998). A new model of thermal diffusion coefficients in binary hydrocarbon mixtures, Ind. And Eng. Chem. Res., Vol. 37, pp. 3331–3342.

Takahashi, R., Sato, S., Sodesawa, T. and Nishida, H. (2002). Effect of pore size on the liquid-phase pore diffusion of nickel nitrate, Phys. Chem. Chem. Phys., Vol. 4, pp. 3800–3805.

Vadasz, P. (2008). *Emerging Topics in Heat and Mass Transfer in Porous Media*, Springer, New York.

Vafai, K. (2000). *Handbook of Porous Media*, Dekker, New York.

Vafai, K. (2005). *Handbook of Porous Media*, Taylor and Francis, Boca Raton.

Appendix

$$g_1 = \mu_d S c_f$$

$$g_2 = \mu_d S c_e$$

$$g_3 = \frac{dP_{B_1}}{dx}$$

$$g_4 = \frac{\varphi}{R_\nu}\frac{dP_{B_2}}{dx}$$

$$g_5 = \frac{\sigma^2}{R_\nu}$$

$$g_6 = \frac{1}{R_{K_T}(h-H)-h}$$

$$g_7 = \frac{c_{a_0}e^{-\mu_d t}}{e^{\sqrt{g_1}\,h} - e^{2\sqrt{g_1}\,H}e^{-\sqrt{g_1}\,h}}$$

$$g_8 = \frac{c_{b_0}e^{-\mu_d t} - e^{-\sqrt{g_2}\,h}}{e^{\sqrt{g_2}\,h} - e^{-\sqrt{g_2}\,h}}$$

$$g_9 = g_3 h - \frac{Gr_1 g_6 R_{K_T}}{6}(3h^2 - 6Hh) - \frac{Gc_1 g_7}{\sqrt{g_1}}(e^{\sqrt{g_1}\,h} + e^{2\sqrt{g_1}\,H}e^{-\sqrt{g_1}\,h})$$

$$g_{10} = \left(\frac{g_4}{g_5} - \frac{Gr_2}{R_\nu g_5} + \frac{Gc_2}{R_\nu(g_2 - g_5)}\right)(-\sqrt{g_5}e^{-\sqrt{g_5}\,h}) + \frac{Gr_2 g_6 h}{R_\nu g_5} - \frac{Gc_2\sqrt{g_2}(g_8 e^{\sqrt{g_2}\,h} - (1-g_8)e^{-\sqrt{g_2}\,h})}{R_\nu(g_2 - g_5)}$$

$$g_{11} = \frac{\frac{R_\mu}{\varphi}\left[g_{14}\sqrt{g_5}(e^{\sqrt{g_5}h} + e^{-\sqrt{g_5}h}) + g_{10}\right] - g_9}{(h-H)}$$

$$g_{12} = \left(\frac{g_4}{g_5} - \frac{Gr_2}{R_\nu g_5} + \frac{Gc_2}{R_\nu(g_2 - g_5)}\right)e^{-\sqrt{g_5}\,h} - \frac{g_4}{g_5} + \frac{Gr_2(g_6 h + 1)}{R_\nu g_5} - \frac{Gc_2(g_8 e^{\sqrt{g_2}\,h} + (1-g_8)e^{-\sqrt{g_2}\,h})}{R_\nu(g_2 - g_5)}$$

$$g_{13} = \frac{g_3 h^2}{2} - \frac{Gr_1 g_6 R_{K_T}}{6}(h^3 - 3Hh^2) - \frac{Gc_1 g_7}{g_1}(e^{\sqrt{g_1}\,h} - e^{2\sqrt{g_1}H}e^{-\sqrt{g_1}h} + \frac{R_\mu}{\varphi}g_{10}$$
$$- g_9 + \left(1 - \frac{g_3 H^2}{2} - \frac{Gr_1 g_6 R_{K_T} H^3}{3}\right)$$

$$g_{14} = \frac{\alpha_p \sigma(g_{12} - g_{13}) - g_{10}}{\sqrt{g_5}(e^{\sqrt{g_5}\,h} + e^{-\sqrt{g_5}\,h})(1 + \frac{\alpha_p \sigma R_\mu}{\varphi}) - \alpha_p \sigma(e^{\sqrt{g_5}\,h} - e^{-\sqrt{g_5}\,h})}$$